MATERIALS SCIENCE / МАТЕРИАЛОВЕДЕНИЕ

UDC 621.762:669.018
DOI 10.17073/0368-0797-2025-3-280-286

Original article
Оригинальная статья

Martensitic transformations in metastable austenitic steel with coarse-grained and ultrafine-grained structure during torsion

N. A. Klevtsova[1], R. Z. Valiev[2], G. V. Klevtsov[1] ✉, M. V. Fesenyuk[3], I. N. Pigaleva[1], V. M. Balashov[1]

[1] **Togliatti State University** (14 Belorusskaya Str., Togliatti, Samara Region 445667, Russian Federation)
[2] **Ufa University of Science and Technology** (12 K. Marksa Str., Ufa, Republic of Bashkortostan 450000, Russian Federation)
[3] **JSC Production Association "Strela"** (26 Shevchenko Str., Orenburg 460005, Russian Federation)

✉ klevtsov11948@mail.ru

Abstract. The *X*-ray method was used to study martensitic transformations in different areas on the fracture surface of the samples made of coarse-grained (CG) and ultrafine-grained (UFG) Fe – 0.02C – 18Cr – 8Ni steel after torsion testing. The fine structure of UFG steel was analyzed on JEM-2100 transmission electron microscope (TEM). The authors carried out the steel hardness tests on TN 300 hardness tester. Static tension of cylindrical samples with a diameter of 3 mm was performed at a temperature of 20 °C on N50KT universal testing machine. Torsion testing of cylindrical samples with a working part diameter of 10 mm and a length of 100 mm was carried out at a temperature of 20 °C using MK-50 unit. The equal-channel angular pressing (ECAP), forming UFG structure, improves the mechanical properties of steel under tension and torsion, and also helps to stabilize the austenitic structure of Fe – 0.02C – 18Cr – 8Ni steel under torsion. 100 % of α-martensite is formed on the fracture surface of CG steel samples, regardless of the *X*-ray diffraction area. On the fracture surface of UFG steel samples, the maximum amount of α-martensite (30 %) is formed in the peripheral area of the fracture; the minimum amount of α-martensite (15 %) – in the fracture central part. The authors made a comparative analysis of the martensitic phases distribution on the samples fracture surface after torsion testing with the martensitic phases distribution in the samples of the same steel after severe plastic deformation by torsion (SPDT), when both ε- and α-martensite are formed. The absence of ε-martensite on the fracture surface of the samples made of CG and UFG Fe – 0.02C – 18Cr – 8Ni steel during torsion is associated with an insignificant pressure for this type of loading, less than in the SPDT process.

Keywords: austenitic steel, torsion testing, fracture, *X*-ray phase analysis, α- and ε-martensite, equal-channel angular pressing (ECAP), severe plastic deformation by torsion (SPDT), coarse-grained (CG) and ultrafine-grained (UFG) structures

For citation: Klevtsova N.A., Valiev R.Z., Klevtsov G.V., Fesenyuk M.V., Pigaleva I.N., Balashov V.M. Martensitic transformations in metastable austenitic steel with coarse-grained and ultrafine-grained structure during torsion. *Izvestiya. Ferrous Metallurgy*. 2025;68(3):280–286. https://doi.org/10.17073/0368-0797-2025-3-280-286

Мартенситные превращения в метастабильной аустенитной стали с крупнозернистой и ультрамелкозернистой структурой при кручении

Н. А. Клевцова[1], Р. З. Валиев[2], Г. В. Клевцов[1] ✉, М. В. Фесенюк[3], И. Н. Пигалева[1], В. М. Балашов[1]

[1] **Тольяттинский государственный университет** (Россия, 445667, Самарская обл., Тольятти, Белорусская ул., 14)
[2] **Уфимский университет науки и технологий** (Россия, 450000, Республика Башкортостан, Уфа, ул. К. Маркса, 12)
[3] **АО ПО «Стрела»** (Россия, 460005, Оренбург, ул. Шевченко, 26)

✉ klevtsov11948@mail.ru

Аннотация. В работе исследованы мартенситные превращения в различных областях поверхности излома образцов из крупнозернистой (КЗ) и ультрамелкозернистой (УМЗ) стали Fe – 0,02C – 18Cr – 8Ni после испытания на кручение. Авторы изучили тонкую структуру УМЗ стали на просвечивающем электронном микроскопе JEM-2100 и провели испытания на твердость с помощью твердомера TN 300. Статическое растяжение цилиндрических образцов диаметром 3 мм выполняли при температуре 20 °C на универсальной

испытательной машине Н50КТ. Испытания на кручение цилиндрических образцов диаметром 10 мм и длиной 100 мм проводили при температуре 20 °С на установке МК-50. Равноканальное угловое прессование, формируя УМЗ структуру, повышает механические свойства стали при растяжении и кручении, а также способствует стабилизации аустенитной структуры стали Fe–0,02C–18Cr–8Ni при кручении. На поверхности изломов образцов из КЗ стали формируется 100 % α-мартенсита. На поверхности изломов образцов из УМЗ стали максимальное количество α-мартенсита (30 %) образуется в периферийной области излома, а минимальное (15 %) – в его центральной части. Авторы провели сравнительный анализ распределения мартенситных фаз на поверхности изломов образцов после испытания на кручение с распределением мартенситных фаз в образцах той же стали после интенсивной пластической деформации кручением (ИПДК), когда образуется как ε-, так и α-мартенсит. Отсутствие ε-мартенсита на поверхности изломов образцов из КЗ и УМЗ стали Fe–0,02C–18Cr–8Ni при кручении авторы связывают с незначительным для данного вида нагружения давлением, меньшем, чем в процессе ИПДК.

Ключевые слова: аустенитная сталь, испытание на кручение, излом, рентгеноструктурный фазовый анализ, α- и ε-мартенсит, равноканальное угловое прессование (РКУП), интенсивная пластическая деформации кручением (ИПДК), крупнозернистая (КЗ) и ультрамелкозернистая (УМЗ) структуры

Для цитирования: Клевцова Н.А., Валиев Р.З., Клевцов Г.В., Фесенюк М.В., Пигалева И.Н., Балашов В.М. Мартенситные превращения в метастабильной аустенитной стали с крупнозернистой и ультрамелкозернистой структурой при кручении. *Известия вузов. Черная металлургия*. 2025;68(3):280–286. https://doi.org/10.17073/0368-0797-2025-3-280-286

Introduction

Austenitic steels, owing to their high mechanical and technological properties, are widely used in medicine, chemical industry, mechanical engineering, instrumentation, and other industrial sectors [1 – 4]. However, certain steels of this class may undergo martensitic transformations when subjected to cooling and deformation. Due to their ambiguous influence on mechanical and physical properties [4 – 6], these transformations hinder reliable prediction of in-service performance and constrain the scope of practical applications.

Metastable austenitic steels are capable of undergoing both $\gamma \rightarrow \alpha$ and $\gamma \rightarrow \varepsilon \rightarrow \alpha$ martensitic transformations. Significant progress has recently been made in understanding the nature of α- and ε-martensite in austenitic steels and alloys [7 – 12]. Martensitic transformations involving the formation of ε-martensite have been most thoroughly investigated in manganese steels and alloys [1; 10 – 12]. In Cr–Ni steels, $\gamma \rightarrow \varepsilon \rightarrow \alpha$ transformation remains poorly understood, as the observed amount of ε-phase usually does not exceed 15 % [11 – 14]. Of particular interest are martensitic transformations in nanostructured metastable austenitic steels with an ultrafine-grained (UFG) structure produced by severe plastic deformation (SPD) methods such as equal-channel angular pressing (ECAP), severe plastic deformation by torsion (SPDT), multi-axial isothermal forging, or other techniques [15]. Martensitic transformations in austenitic steels under ECAP and SPDT have been addressed, for example, in [4; 16; 17]. In particular, it has been noted [17] that under certain SPDT conditions involving high hydrostatic pressure, not only direct but also reverse martensitic transformations can occur in metastable austenitic steels.

When assessing the potential applications of austenitic Cr–Ni steels with a UFG structure in medicine, it is important to consider that many implantable devices (screws, pins, and similar components) are subjected to torsional loading in service. The formation of martensitic phases during SPD or under operational conditions may affect not only the strength characteristics of such devices but also the biocompatibility of the material. However, the effect of martensitic-phase formation on the properties of UFG austenitic steels under torsion remains insufficiently explored. A more detailed investigation into martensitic transformations under torsion in UFG steels may provide a deeper understanding of the physical nature and mechanisms of such transformations in steels of this class under various types of mechanical loading.

The objective of this study is to evaluate the influence of different SPD techniques – specifically, ECAP and SPDT – on the mechanism of martensitic transformations in austenitic Cr–Ni steel, and to establish a correlation between the intensity of these transformations and the fracture behavior of both CG and UFG steels subjected to torsion.

Materials and methods

The material selected for this study was austenitic Fe–0.02C–18Cr–8Ni steel (wt. %: 0.023 C; 17.95 Cr; 7.95 Ni; 1.85 Mn; 0.6 Cu; 0.38 Si; 0.35 Mo; 0.15 Co). The steel was examined in two structural states: the initial CG condition, obtained by water quenching from 1050 °C with a 1 h hold, and the UFG condition produced via ECAP. The ECAP process was carried out following quenching under the aforementioned conditions at a temperature of 350 °C using route *Bc*, with four passes and a channel angle of $\varphi = 1200$ [15].

The CG structure was examined using an Axiovert 40 MAT optical microscope, while the fine structure of the UFG steel was analyzed by transmission electron microscopy (TEM) on a JEM-2100 microscope. Hardness measurements were performed on a TN 300 hardness tester. Uniaxial tensile tests of cylindrical samples (3 mm in diameter) were conducted at 20 °C

using an N50KT universal testing machine. Torsion testing of cylindrical samples with a working section diameter of 10 mm and a length of 100 mm was carried out at 20 °C using the MK-50 unit, in accordance with GOST 3565–80 and GOST R 50581–93 (ISO 6475–89). Based on torque–twist angle diagrams, the ultimate shear strength (τ_k), yield strength ($\tau_{0.3}$), and shear strain (g) were determined as described in [18]. Fractographic examination of the fracture surfaces was performed using a JCM-6000 scanning electron microscope (SEM) (EOL Ltd., Japan).

The volume fraction of martensitic phases in the effectively diffracting surface layer of the material, in different areas of the sample surface or fracture surface, was determined based on the integrated intensity of (111) K_α diffraction line of the γ-phase, (110) K_α line of the α-phase, and (101) K_α line of the ε-phase [5; 19]. The selection of these diffraction lines is based on their association with single-variant phase transformations. In such transformations, the orientation of the matrix phase after transformation produces new phases with orientations that are largely represented by the chosen lines [20], which minimizes the influence of crystallographic texture on the intensity ratio of the corresponding peaks. The percentage content of γ-austenite, α-martensite, and ε-martensite was calculated using the formulas [5; 19]:

$$V_\gamma = \frac{C_1 I_{111_\gamma}}{C_1 I_{111_\gamma} + C_2 I_C + C_3 I_{101_\varepsilon}} \cdot 100\ \%;$$

$$V_\alpha = \frac{C_2 I_C - C_4 I_{101_\varepsilon}}{C_1 I_{111_\gamma} + C_2 I_C + C_3 I_{101_\varepsilon}} \cdot 100\ \%;$$

$$V_\varepsilon = \frac{C_5 I_{101_\varepsilon}}{C_1 I_{111_\gamma} + C_2 I_C + C_3 I_{101_\varepsilon}} \cdot 100\ \%.$$

The coefficients $C_1 \ldots C_5$ for FeK_α radiation are given in Table 1. The values, I_{111_γ}, I_{101_ε} and $I_C = I_{110_\alpha} + I_{002_\varepsilon}$ represent the integrated intensity of the corresponding diffraction lines (in the latter case, (110) K_α line of the α-phase overlaps with (002) K_α line of the ε-phase).

X-ray phase analysis of the fracture surfaces, which exhibit surface roughness and a certain degree of crystal lattice distortion, resulted in broadening of the diffraction lines. In some cases, this caused incomplete separation of (110) K_α line of the α-phase and (111) K_α line of the γ-phase. In such cases, graphical separation of the overlapping peaks was performed based on the assumption of line symmetry [19]. *X*-ray diffraction of sample surfaces and fracture surfaces was performed using a DRON-2.0 diffractometer (U = 22 kV, I = 8 mA) with FeK_α radiation.

Table 1. **Coefficients for calculating the volumetric phase content for FeK_α radiation**

Таблица 1. **Коэффициенты для расчета объемного содержания фаз для FeK_α-излучения**

Radiation type	C_1	C_2	C_3	C_4	C_5
FeK_α	2.459	1.799	2.025	0.444	2.469

Research results

Structure and mechanical properties of Fe – 0.02C – 18Cr – 8Ni steel

In the initial state, Fe–0.02C–18Cr–8Ni steel exhibited a single-phase γ-austenite structure with an average grain size of 30 μm (Fig. 1, *a*). After ECAP, an elongated banded UFG structure was observed. On the background of a developing cell substructure, microbands and shear bands were present (Fig. 1, *b*). Within the mesobands, a high dislocation density was observed, including dislocation clusters and tangles. The average grain size was 0.55 μm. *X*-ray phase analysis confirmed that after ECAP, the steel retained a single-phase γ-austenite structure. The mechanical properties of the steel under uniaxial tension and torsion are summarized in Table 2.

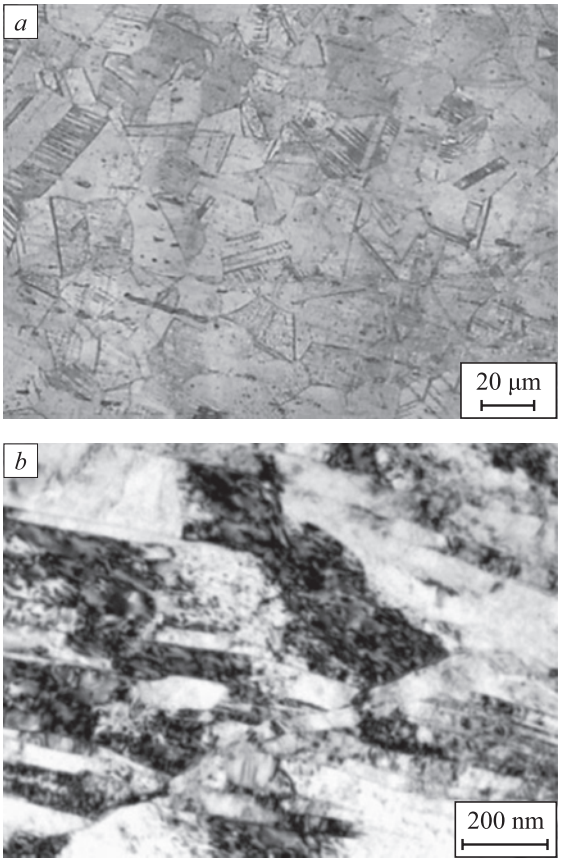

Fig. 1. Microstructure of CG (*a*) and UFG (*b*) Fe–0.02C–18Cr–8Ni steel

Рис. 1. Микроструктура стали Fe–0,02C–18Cr–8Ni в КЗ (*a*) и УМЗ (*b*) состоянии

Table 2. **Average grain size and mechanical properties of CG and UFG Fe–0.02C–18Cr–8Ni steel at tension and torsion**

Таблица 2. **Средний размер зерна и механические свойства стали Fe–0,02C–18Cr–8Ni в КЗ и УМЗ состоянии при растяжении и кручении**

Structural state	d_{avg}, μm	Hardness, HB	Tensile properties			Torsion properties		
			σ_u, MPa	$\sigma_{0.2}$, MPa	δ, %	τ_k, MPa	$\tau_{0.3}$, MPa	g, %
CG (initial)	30,00	159	624 ± 6	283 ± 8	65 ± 0.7	688 ± 8	194 ± 10	89 ± 3
UFG (after ECAP)	0.55	363	1112 ± 8	1065 ± 15	20 ± 0.5	917 ± 10	740 ± 15	37 ± 1

Martensitic transformations on the fracture surfaces of Fe – 0.02C – 18Cr – 8Ni steel under torsion

Fracture of both CG and UFG steel samples under torsion occurred via a shear mechanism. The average roughness of the fracture surfaces for CG and UFG samples was nearly identical (Fig. 2, *a*, *e*). All fracture surfaces exhibited three characteristic zones: a relatively smooth peripheral area, a transitional (middle) area, and a ductile central area with a pronounced rough macroscopic

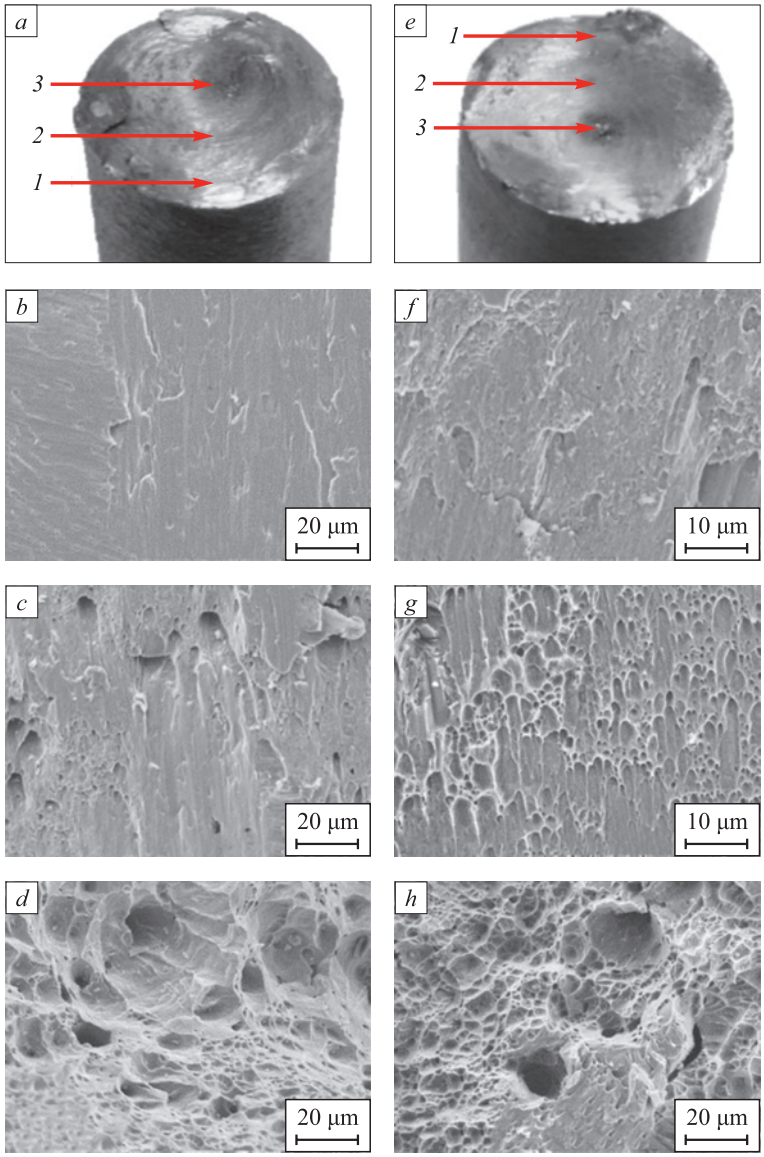

Fig. 2. Torsional general form (*a*, *e*) and fracture surface microrelief (*b – d*, *f – h*) of the samples from CG (*a – d*) and UFG (*e – h*) Fe–0.02C–18Cr–8Ni steel. Microrelief was taken from peripheral part *1* (*b*, *f*), middle part *2* (*c*, *g*) and central part *3* (*d*, *h*)

Рис. 2. Общий вид (*a*, *e*) и микрорельеф (*b – d*, *f – h*) изломов на кручение образцов из КЗ (*a – d*) и УМЗ (*e – h*) стали Fe–0,02C–18Cr–8Ni. Микрорельеф получен с периферийной зоны *1* (*b*, *f*), переходной зоны *2* (*c*, *g*) и центральной зоны *3* (*d*, *h*)

relief (Fig. 2, *a*, *e*). In the peripheral area, the micromorphology was weakly developed (Fig. 2, *d*, *h*), formed as a result of mutual friction between the opposing fracture surfaces. The middle area was dominated by shear dimples (Fig. 2, *c*, *g*), which appeared more pronounced on the fracture surface of the UFG steel. In the central area, regardless of structural state, the micromorphology consisted of equiaxed dimples formed by microvoid coalescence (Fig. 2, *d*, *h*).

X-ray phase analysis revealed that, on the fracture surface of CG steel samples failed under torsion, 100 % α-martensite was formed regardless of the *X*-ray scanning area (Table 3). On the fracture surfaces of UFG steel samples, the maximum amount of α-martensite (30 %) was detected in the peripheral area, while the minimum amount (15 %) was observed in the central area of the fracture surface (Table 3). No ε-martensite was detected on any of the examined fracture surfaces.

Thus, ECAP, by producing a UFG structure, enhances the mechanical properties of Fe–0.02C–18Cr–8Ni steel under both tension and torsion and contributes to the stabilization of its austenitic structure under torsion. As a result of plastic deformation under torsion, the austenitic steel undergoes γ → α martensitic transformations.

Discussion

The results of the present study demonstrate that nanostructuring of Fe–0.02C–18Cr–8Ni steel by ECAP, which produces a UFG structure, not only improves the tensile and torsional strength of the material (Table 2), but also contributes to the stabilization of the austenitic structure under torsion (Table 3). Fracture of CG steel samples under torsion, regardless of the failure mechanism, resulted in the formation of 100 % α-martensite on the fracture surface. In the UFG samples, the maximum amount of α-martensite was observed in the peripheral and transitional areas of the fracture surface, where shear dimples and areas of mutual friction between opposing fracture surfaces predominated. The minimum amount of α-martensite was found in the central area, where tensile dimples were dominant (Fig. 2).

It is of particular interest to compare the formation mechanism and distribution of martensitic phases on the fracture surfaces of UFG Fe–0.02C–18Cr–8Ni steel samples after torsion testing with the distribution of martensitic phases in samples of the same steel subjected to severe plastic deformation by torsion (SPDT). In the latter case, similar shear stresses are generated, but additional compressive stresses are also applied [15]. As noted in [4], the phase composition of Fe–0.02C–18Cr–8Ni steel was studied on samples with a diameter of 20 mm subjected to SPDT at a pressure of 6 GPa and 2 full revolutions. The grain size in the UFG structure after SPDT in the mid-radius area was 0.20 – 0.25 μm. After SPDT, the surface roughness across the entire sample diameter was nearly uniform. However, the microhardness showed significant radial inhomogeneity, ranging from 350 HV at the center to 550 – 600 HV at the periphery [4]. *X*-ray phase analysis was performed in the peripheral, transitional, and central areas of the sample surface after SPDT. The analysis revealed the presence of both α- and ε-martensite. The highest amount of ε-martensite (about 11 %) was found in the central area, while no ε-martensite was detected in the peripheral area [4] (Table 4).

Martensitic transformations on the fracture surfaces of CG and UFG steel samples under torsion occur in the absence of significant compressive stresses. As a result, the transformation of austenite proceeds to completion, forming α-martensite. In contrast, SPDT involves not only torsional deformation but also the application of high compressive stresses (6 GPa). This high pressure, especially in the central area of the sample [15], promotes the γ → ε transformation but suppresses the ε → α transformation due to the difference in specific volumes between the FCC, HCP, and BCC crystal structures. Therefore, in the central and partially in the transitional areas, both α- and ε-martensite are detected by *X*-ray phase analysis. In the peripheral area, owing to the more distorted crystal structure and the relatively lower compressive stress, only α-martensite

Table 3. **Amount of α-martensite in different parts on fracture surface of the samples made of Fe–0.02C–18Cr–8Ni steel at torsion, %**

Таблица 3. **Количество α-мартенсита в различных участках на поверхности изломов, полученных при кручении образцов из стали Fe–0,02C–18Cr–8Ni, %**

Structural state	*X*-ray scanning area		
	peripheral	transitional	central
CG (initial)	100	100	100
UFG (after ECAP)	30	23	15

Table 4. **Amount of α- and ε-martensite in different parts on surface of the samples made of Fe–0.02C–18Cr–8Ni steel after HPDT [4], %**

Таблица 4. **Количество α- и ε-мартенсита в различных участках на поверхности образцов из стали Fe–0,02C–18Cr–8Ni после ИПДК [4], %**

Type of martensite	*X*-ray scanning area		
	peripheral	transitional	central
α-martensite	37	36	28
ε-martensite	0	3	11

is formed (Table 4). This interpretation is supported by the fact that the combined amount of ε- and α-martensite across all areas of the sample after SPDT totals 37 – 39 % (Table 4).

Conclusions

Equal-channel angular pressing, through the formation of a UFG structure, enhances the strength characteristics of austenitic Fe – 0.02C – 18Cr – 8Ni steel under both tension and torsion, while also increasing the stability of its austenitic phase against martensitic transformation during torsion.

In CG steel samples, fracture under torsion – regardless of the failure mechanism – results in the formation of 100 % α-martensite across the entire fracture surface. In UFG steel samples, the highest amount of α-martensite (30 %) is formed in the peripheral area of the fracture surface, where shear dimples and frictional features dominate. The lowest amount of α-martensite (15 %) is observed in the central area, characterized primarily by tensile dimples.

The absence of ε-martensite on the fracture surfaces of both CG and UFG samples under torsion is attributed to the relatively low compressive stress associated with this type of loading, which is insufficient to induce γ → ε transformation. In contrast, under SPDT, where compressive pressures reach approximately 6 GPa, *X*-ray phase analysis confirms the presence of ε-martensite in this steel.

References / Список литературы

1. Sagaradze V.V., Uvarov A.I. Strengthening and Properties of Austenitic Steels. Yekaterinburg, RIO UB RAS; 2013:720. (In Russ.).

   Сагарадзе В.В., Уваров А.И. Упрочнение и свойства аустенитных сталей. Екатеринбург: РИО УрО РАН; 2013:720.
2. Klevtsov G.V., Valiev R.Z., Fesenyuk M.V., Klevtsova N.A., Tyur'kov M.N., Abramova M.M., Raab G.I. Strength and fracture mechanism during torsion of ultrafine-grained austenitic steel for medical applications. *Izvestiya. Ferrous Metallurgy*. 2021;64(11):832–838. (In Russ.). https://doi.org/10.17073/0368-0797-2021-11-832-838

   Клевцов Г.В., Валиев Р.З., Фесенюк М.В., Клевцова Н.А., Тюрьков М.Н., Абрамова М.М., Рааб Г.И. Прочность и механизм разрушения при кручении ультрамелкозернистой аустенитной стали медицинского назначения. *Известия вузов. Черная металлургия*. 2021;64(11):832–838. https://doi.org/10.17073/0368-0797-2021-11-832-838
3. Vologzhanina S.A., Igolkin A.F., Peregudov A.A. Research of properties of austenitic steels. *Key Engineering Materials*. 2021;(887):242–246. https://doi.org/10.4028/www.scientific.net/KEM.887.242
4. Klevtsov G.V., Valiev R.Z., Klevtsova N.A., Enikeev N.A., Pigaleva I.N., Abramova M.M., Frolova O.A. Effect of severe plastic deformation on martensitic transformations in a metastable austenitic steel. *Letters on Materials*. 2023;13(4s):397–402.
5. Klevtsova N.A., Frolova O.A., Klevtsov G.V. Fracture of Austenitic Steels and Martensitic Transformations in Plastic Zones. Moscow: Akademiya Estestvoznaniya; 2005:155. (In Russ.).

   Клевцова Н.А., Фролова О.А., Клевцов Г.В. Разрушение аустенитных сталей и мартенситные превращения в пластических зонах. Москва: Академия Естествознания; 2005:155.
6. Lecroisey F., Pineau A. Martensitic transformations induced by plastic deformation in the Fe–Ni–Cr–C system. *Metallurgical Transactions*. 1972;3:387–396. https://doi.org/10.1007/BF02642042
7. Ullrich C., Eckner R., Krüger L., Martin S., Klemm V., Rafaja D. Interplay of microstructure defects in austenitic steel with medium stacking fault energy. *Materials Science and Engineering: A*. 2016;649:390–399. https://doi.org/10.1016/j.msea.2015.10.021
8. Das A. Magnetic properties of cyclically deformed austenite. *Journal of Magnetism and Magnetic Materials*. 2014;361: 232–242. https://doi.org/10.1016/j.jmmm.2014.02.006
9. Park M.C., Yun J.Y., Shin G.S., Kim S.J. Strain-induced α′ε-martensitic transformation behavior and solid particle erosion resistance of austenitic Fe–Cr–C–Mn–Ni alloys. *Tribology Letters*. 2014;54(1):51–58. https://doi.org/10.1007/s11249-014-0306-3
10. Korshunov L.G., Chernenko N.L. Effect of γ→e martensitic transformation the tribological properties of chromium–manganese austenitic steels. *Diagnostics, Resource and Mechanics of Materials and Structures*. 2019;(5):48–59. https://doi.org/10.17804/2410-9908.2019.5.048-059
11. Hans-Jocnen V. Mechanische Eigenschaften austenitischer, kohlenstoffarmer Cr–Ni–Stahl. *Neue Hutte*. 1970;15(4): 234–237. (In Germ.).
12. Bhattacharya K. Microstructure of Martensite: Why It Forms and How It Gives Rise to the Shape-Memory Effect: Oxford Series on Materials Modelling. Oxford University Press; 2004:323.
13. Otsuka K., Ren X. Mechanism of martensite aging effects and new aspects. *Materials Science and Engineering: A*. 2001;312(1-2):207–218. https://doi.org/10.1016/S0921-5093(00)01877-3
14. Cakmak E., Vogel S., Choo H. Effect of martensitic phase transformation on the hardening behavior and texture evolution in a 304L stainless steel under compression at liquid nitrogen temperature. *Materials Science and Engineering: A*. 2014;589:235–241. http://dx.doi.org/10.1016/j.msea.2013.09.093
15. Valiev R.Z., Zhilyaev A.P., Langdon T.G. Bulk Nanostructured Materials: Fundamentals and Applications. Hoboken, New Jersey: John Wiley & Sons; 2014:440.
16. Li J.G., Umemoto M., Todaka Y., Fujisaku K., Tsuchiya K. The dynamic phase transformation and formation of nanocrystalline structure in SUS304 austenitic stainless steel subjected to high pressure torsion. *Reviews on Advanced Materials Science*. 2008;18:577–582.
17. Litovchenko I.Yu., Tyumentsev A.N., Zahozheva M.I., Korznikov A.V. Direct and reverse martensitic transforma-

tion and formation of nanostructured states during severe plastic deformation of metastable austenitic stainless steel. *Reviews on Advanced Materials Science*. 2012;31:47–53.

18. Zolotorevskii V.S. Mechanical Properties of Metals. Moscow: MISIS; 1998:400. (In Russ.).

Золоторевский В.С. Механические свойства металлов. Москва: МИСИС; 1998:400.

19. R 50-54-52/2-94. Strength calculations and tests. Method of *X*-ray structural analysis of fractures. Determination of fracture characteristics of metallic materials by the *X*-ray method. Moscow: VNIINMASH of the State Standard of Russia; 1994:28. (In Russ.).

Р 50-54-52/2-94. Расчеты и испытания на прочность. Метод рентгеноструктурного анализа изломов. Определение характеристик разрушения металлических материалов рентгеновским методом. Москва: ВНИИНМАШ Госстандарта России; 1994:28.

20. Ageev N.V., Babareko A.A., Betzofen S.Ya. Texture description using the inverse pole figures method. *Izvestiya of the USSR Academy of Sciences. Metals*. 1974;(1):94–97. (In Russ.).

Агеев Н.В., Бабарэко А.А., Бецофен С.Я. Описание текстуры методом обратных полюсных фигур. *Известия АН СССР. Металлы*. 1974;(1):94–97.

Information about the Authors / Сведения об авторах

Natal'ya A. Klevtsova, *Dr. Sci. (Eng.), Assist. Prof., Prof. of the Chair of Nanotechnology, Materials and Mechanics*, Togliatti State University
ORCID: 0000-0001-8667-656X
E-mail: inshtet@mail.ru

Ruslan Z. Valiev, *Dr. Sci. (Phys.-Math.), Prof., Director of the Research Institute of Physics of Advanced Materials*, Ufa University of Science and Technology
ORCID: 0000-0003-4340-4067
E-mail: rzvaliev@yahoo.com

Gennadii V. Klevtsov, *Dr. Sci. (Eng.), Prof. of the Chair of Nanotechnology, Materials and Mechanics*, Togliatti State University
ORCID: 0000-0002-4928-7415
E-mail: klevtsov11948@mail.ru

Maksim V. Fesenyuk, *Cand. Sci. (Eng.), Head of the Division*, JSC Production Association "Strela"
ORCID: 0000-0002-4584-6638
E-mail: maksim_fesenyuk@mail.ru

Irina N. Pigaleva, *Head of Laboratories of the Chair of Nanotechnology, Materials and Mechanics*, Togliatti State University
E-mail: irina1.985@mail.ru

Vadim M. Balashov, *MA Student of the Chair of Nanotechnology, Materials and Mechanics*, Togliatti State University
E-mail: zeus348@mail.ru

Наталья Артуровна Клевцова, *д.т.н., доцент, профессор кафедры нанотехнологий, материаловедения и механики*, Тольяттинский государственный университет
ORCID: 0000-0001-8667-656X
E-mail: inshtet@mail.ru

Руслан Зуфарович Валиев, *д.ф-м.н., профессор, директор НИИ физики перспективных материалов*, Уфимский университет науки и технологий
ORCID: 0000-0003-4340-4067
E-mail: rzvaliev@yahoo.com

Геннадий Всеволодович Клевцов, *д.т.н., профессор кафедры нанотехнологии, материаловедения и механики*, Тольяттинский государственный университет
ORCID: 0000-0002-4928-7415
E-mail: klevtsov11948@mail.ru

Максим Викторович Фесенюк, *к.т.н., начальник отдела*, АО «ПО «Стрела»
ORCID: 0000-0002-4584-6638
E-mail: maksim_fesenyuk@mail.ru

Ирина Николаевна Пигалева, *заведующий лабораториями кафедры нанотехнологии, материаловедения и механики*, Тольяттинский государственный университет
E-mail: irina1.985@mail.ru

Вадим Михайлович Балашов, *магистрант кафедры нанотехнологии, материаловедения и механики*, Тольяттинский государственный университет
E-mail: zeus348@mail.ru

Contribution of the Authors / Вклад авторов

N. A. Klevtsova – planning and organizing the experiment, writing the text.
R. Z. Valiev – obtaining steel in UMP condition.
G. V. Klevtsov – *X*-ray structural phase analysis of steel fracture surfaces.
M. V. Fesenyuk – conducting torsion testing of the samples.
I. N. Pigaleva – manufacturing and preparation of the samples from CG and UFG steel for testing.
V. M. Balashov – calculation of strength properties of CG and UFG steel and phase composition under torsion.

Н. А. Клевцова – планирование и организация эксперимента, оформление статьи.
Р. З. Валиев – получение стали в УМЗ состоянии.
Г. В. Клевцов – рентгеноструктурный фазовый анализ поверхности изломов стали.
М. В. Фесенюк – проведение испытания образцов на кручение.
И. Н. Пигалева – изготовление и подготовка образцов из КЗ и УМЗ стали для испытания.
В. М. Балашов – расчет прочностных свойств КЗ и УМЗ стали и фазового состава при кручении.

Received 21.12.2024
Revised 11.03.2025
Accepted 23.04.2025

Поступила в редакцию 21.12.2024
После доработки 11.03.2025
Принята к публикации 23.04.2025